Elimination of the Hydrolytic Water Molecule in a Class A β-Lactamase Mutant: Crystal Structure and Kinetics[†,‡]

Laura E. Zawadzke, Celia C. H. Chen, Soojay Banerjee, Zhong Li, Susana Wäsch, Geeta Kapadia, John Moult, and Osnat Herzberg*

Center for Advanced Research in Biotechnology, University of Maryland Biotechnology Institute, 9600 Gudelsky Drive, Rockville, Maryland 20850

Received September 5, 1996; Revised Manuscript Received October 17, 1996[⊗]

ABSTRACT: Two site-directed mutant enzymes of the class A β-lactamase from *Staphylococcus aureus* PC1 were produced with the goal of blocking the site that in the native enzyme is occupied by the proposed hydrolytic water molecule. The crystal structures of these two mutant enzymes, N170Q and N170M, have been determined and refined at 2.2 and 2.0 Å, respectively. They reveal that the side chain of Gln170 displaces the water molecule, whereas that of Met170 does not. In both cases, the catalytic rates with benzylpenicillin are reduced by 10^4 compared with the native enzyme. With nitrocefin, the N170Q mutant enzyme exhibits an approximately 800-fold reduced rate compared with the native enzyme and in addition, a fast initial burst with stoichiometry of 1 mol of degraded nitrocefin/mol of enzyme. Stopped-flow kinetic experiments establish that the rate constant of the burst is 250 s^{-1}, a value comparable with the rate of acylation of the native enzyme. Two structurally based mechanisms that explain the kinetic properties of the N170Q β-lactamase are proposed, both invoking a deacylation-impaired enzyme due to the elimination of the hydrolytic water molecule. The catalytic rate of the N170M mutant enzyme with nitrocefin is reduced by approximately 50-fold compared with the native enzyme, and the slow progressive inhibition that is revealed indicates that the hydrolysis proceeds via a branched pathway mechanism. This is consistent with the structural data that show that the water site is preserved and that Met170 occupies part of the space that is required for substrate binding. The short contacts between the substrate and the enzyme may lead to structure perturbation and inactivation.

The class A, C, and D β-lactamases are enzymes that utilize a serine residue to hydrolyze β-lactam antibiotics by a mechanism that involves a seryl acyl intermediate. As with the serine proteases, the process can be divided into acylation and deacylation steps. In addition to the catalytic serine [Ser70 in the consensus numbering scheme for the class A enzymes (Ambler, 1980; Ambler et al., 1991)], the serine β-lactamases also share an invariant lysine (Lys73 in the class A enzymes). Crystal structures of class A and class C β-lactamases show this lysine in close proximity to the catalytic serine (Herzberg & Moult, 1987; Herzberg, 1991; Moews et al., 1990; Knox & Moews, 1991; Jelsch et al., 1992, 1993; Strynadka et al., 1992; Ofner et al., 1990; Lobkovsky et al., 1993). In addition, Ser130 in the class A β-lactamases, and its counterpart in the class C enzymes, Tyr150, also interacts with the catalytic serine. Herzberg and Moult (1987) observed that the position of the lysine is analogous to that of the histidyl residue in the catalytic triad of the serine proteases and proposed that it assists proton transfer during acylation from the hydroxyl group of Ser70 to the nitrogen atom of the β-lactam. On the other hand, Ofner et al. (1990) and Lobkovsky et al. (1994) suggested that in the class C enzymes the general base during both acylation and deacylation is Tyr150 rather than the lysine residue. Mutagenesis data are consistent with a catalytic role for Lys73 (Gibson et al., 1990; Tsukamoto et al., 1990; Monnaie et al., 1994; Chen et al., 1996), the nature of which is still unclear and controversial (Herzberg & Moult, 1991; Strynadka et al., 1992; Gibson et al., 1990; Lamotte-Brasseur et al., 1991; Damblon et al., 1996).

Another analogy to the serine proteases is offered by the presence of an oxyanion hole that helps stabilize the negatively charged tetrahedral transition state. Crystal structures of acyl enzymes (Chen & Herzberg, 1992; Strynadka et al., 1992) and of a tetrahedral transition state analog (Chen et al., 1993; Lobkovsky et al., 1994) revealed the expected interaction of the substrate/inhibitors with the oxyanion hole in both class A and class C enzymes.

In contrast with the serine proteases, the structural information available for the class A β-lactamases indicates that the acylation step is assisted by different catalytic machinery than that assisting deacylation. The class A enzymes contain a water molecule that forms electrostatic interactions with the invariant Ser70 and with two residues located on a Ω-loop, Glu166 and Asn170. It has been proposed that the interaction with Glu166 enhances the nucleophilicity of this water molecule, preparing it for deacylation of the enzyme (Herzberg & Moult, 1987, 1991). When compared with the direction of attack proposed for the hydrolytic water in the serine proteases, the deacylating water in the class A β-lactamases attacks from the opposite direction. Notably, the class C β-lactamases lack the Ω-loop, and there is no carboxylate group appropriately positioned

[†] Supported by NIH Grant RO1-AI27175.

[‡] The coordinates of the N170Q and N170M β-lactamase structures have been deposited in the Brookhaven Protein Data Bank (filenames 1KGF and 1KGE).

* To whom correspondence should be addressed (telephone, 301-738-6245; fax, 301-738-6255; E-mail, osnat@elan1.carb.nist.gov).

[⊗] Abstract published in *Advance ACS Abstracts,* December 1, 1996.

S0006-2960(96)02242-8 CCC: $12.00

Table 1: Oligonucleotides Used for PCR Mutagenesis and DNA Sequencing

no.	oligonucleotide	sequence (5′ → 3′)	purpose
1	LZBAMHI	GTCCGGCGTAGAGGATCCGGAATTCTCATG	PCR
2	TSHIND3	ATCAGTTTTTGATATCAAGCTTATACATGTCAACG	PCR
3	LZN170Q1	GAGATAGAATTACAGTACTATTCACC	PCR
4	LZN170Q2	GGTGAATAGTACTGTAATTCTATCTC	PCR
5	LZN170M1	GAGATAGAATTAATGTACTATTCACC	PCR
6	LZN170M2	GGTGAATAGTACATTAATTCTATCTC	PCR
7	SEQ420	CTAAAATAGGAGAATAAGCAAC	sequencing
8	SEQ534	AACTTTTTTGATTCCACCGATTTC	sequencing
9	SEQ652	ACCGAAAGCAGCAGGTGTTGAAG	sequencing
10	SEQ831	ACATCATTTCTAGAAGCATATGT	sequencing

in the active site to activate a water molecule. As mentioned above, the nucleophilicity of the hydrolytic water is therefore thought to be enhanced by Tyr150. Hence, despite the intriguing structural similarities between the two classes of serine β-lactamases, they appear to have evolved with two distinct catalytic machineries.

Mutagenesis and crystallographic studies support the proposal that the role of Glu166 is predominantly during deacylation. In the P54 mutant enzyme from *Staphylococcus aureus* PC1, Glu166 is conformationally disordered, and deacylation becomes the rate-limiting step (Herzberg et al., 1991). In the *Escherichia coli* TEM-1 and *Bacillus licheniformis* β-lactamases, replacement of Glu166 by a noncharged residue resulted in accumulation of the acyl enzyme intermediate (Adachi et al., 1991; Escobar et al., 1991). One of these mutant enzymes (E166N) was used to determine the crystal structure of an acyl enzyme of the TEM-1 β-lactamase (Strynadka et al., 1992). Despite these data, Gibson et al. (1990) and Lamotte-Brasseur et al. (1991) proposed that Glu166 acts as the general base during both the acylation and deacylation steps, with the proton first being transferred from Ser70 to the carboxylate group via the bridging water molecule. Structural considerations make it difficult to envisage how the proton would next be transferred to the substrate, because Glu166 is remote from the β-lactam's nitrogen atom and on the opposite side relative to the hydroxyl group of Ser70. This is substantiated by the various crystal structures of substrate/inhibitor complexes.

The above data pertain to the role of Glu166 and provide compelling, if indirect, evidence about the identity of the hydrolytic water molecule. In the current study, the identity of this water molecule has been directly examined by employing site-directed mutagenesis, using the expression system for β-lactamase from *S. aureus* PC1 (Zawadzke et al., 1995). Asn170, an amino acid residue that interacts with the postulated hydrolytic water molecule, has been replaced by amino acids with larger side chains, so as to block the niche where the water molecule is normally accommodated. Mutants that displace the hydrolytic water molecule would be expected to be deacylation-defective and to exhibit burst kinetics characteristics. Two mutant enzymes have been prepared. One contains a glutamine at position 170, a conservative replacement in terms of polarity and functional group. The second contains a methionine, a more hydrophobic side chain compared with the parent asparagine residue. The engineering of two functionally different residues was carried out because it was not obvious whether or not the conformation in which the side chain occupies the water molecule site would be adopted. Instead, one of these side chains could protrude into the active site depression impairing substrate binding. The X-ray structures and kinetic data presented here reveal that displacement of the water molecule was achieved with the N170Q β-lactamase and that the enzyme is deacylation-impaired. The water molecule is still present in the structure of the N170M mutant enzyme. Deacylation is impaired, but the kinetics are complex.

MATERIALS AND METHODS

Materials, Mutagenesis, and Protein Purification. The *S. aureus* PC1 β-lactamase mutants were engineered, expressed in the *E. coli* TG1, and purified as described previously (Zawadzke et al., 1995), with the following changes: The polymerase chain reaction (PCR) mutagenesis was performed using the Vent(exo$^-$) DNA polymerase from New England Biolabs (Beverly, MA). The template plasmid, pTS32, was purified with the Qiagen Maxi plasmid kit (Chatsworth, CA) and used in DNA sequencing and PCR mutagenesis.

The four-primer overlap−extension method (Ho et al., 1989) was used to produce single-site mutants from the β-lactamase gene on pTS32 (*bla*Z). The oligonucleotides used are shown in Table 1. The external primers were oligonucleotides 1 and 2, and their respective internal mutagenic primers were oligonucleotides 3 and 4 for the N170Q replacement and 5 and 6 for the N170M replacement. The single-site DNA mutant *bla*Z genes were resequenced using double-strand plasmid DNA with either the Sequenase Quick-Denature plasmid DNA sequencing kit or the Sequenase 2.0 kit (United States Biochemicals, Cleveland, OH), following the manufacturer's protocol for denaturing the double-strand DNA. Sequencing oligonucleotides are also presented in Table 1. The LZN170M1 and LZN170M2 oligonucleotides not only substitute a methionine for asparagine at amino acid 170 but also incorporate a third *Ase*I restriction enzyme site on the plasmid. The engineered gene includes an additional N-terminal methionine compared with the native amino acid sequence.

Enzyme Assay and Kinetics. The benzylpenicillin was purchased from Sigma (St. Louis, MO), and the nitrocefin was purchased from Unipath (Ogdensburg, NY). 6-β-[(Furylacryloyl)amido]penicillanic acid triethylamine salt (FAP) was purchased from Calbiochem (La Jolla, CA). Steady-state kinetic measurements were made on either a Varian Cary 4 spectrophotometer or a Hewlett-Packard 8452A diode array spectrophotometer. Stopped-flow analysis was carried out on a Kintek SF-2001 from Kintek Instruments (University Park, PA). All assays were performed at 25 °C in solutions containing 0.1 M potassium phosphate buffer at pH 6.8.

Substrate hydrolysis was monitored by loss of absorbance at 232 and 344/345 nm for benzylpenicillin and FAP,

Table 2: Data Processing Statistics for the N170Q and N170M β-Lactamases

	N170Q	N170M
space group	*I*222	*I*222
unit cell parameters (Å)	$a = 54.3$, $b = 94.8$, $c = 140.5$	$a = 54.3$, $b = 94.0$, $c = 139.2$
resolution (Å)	2.2	2.0
no. of observations	28166	89328
no. of unique reflections	16464	19020
completeness[a]	0.87 (0.76)	0.79 (0.42)
fraction with $I \geq 2\sigma(I)$[a]	0.78 (0.45)	0.78 (0.62)
R_{sym}[a,b]	0.079 (0.215)	0.090 (0.347)

[a] The values in parentheses are for the highest 0.1 Å resolution shell. [b] $R_{sym} = \sum_h \sum_i |\langle I(h)\rangle - I(h)_i| / \sum_h \sum_i I(h)_i$ for symmetry-related observations.

respectively, and by increase in absorbance at 500 nm for nitrocefin. The extinction coefficients used were as follows: benzylpenicillin, $\Delta\epsilon_{232} = 940$ M^{-1} cm^{-1}; nitrocefin, $\Delta\epsilon_{500} = 15\,900$ M^{-1} cm^{-1}; FAP, $\Delta\epsilon_{344} = 1330$ M^{-1} cm^{-1} (Hewlett-Packard), $\Delta\epsilon_{345} = 1170$ M^{-1} cm^{-1} (Varian Cary 4). Enzyme concentrations were determined using $\epsilon_{280} = 19\,500$ M^{-1} cm^{-1} (Carrey & Pain, 1978). Kinetic analysis was performed with the use of the program SigmaPlot by Jandel Scientific.

Crystallization and X-ray Data Collection. Crystals of the N170M and N170Q β-lactamases were grown at room temperature by the vapor-diffusion method in hanging drops, equilibrated against reservoir solutions containing 84% saturated ammonium sulfate, 0.4% w/v dimethylpoly(ethylene glycol) 2000 (for N170Q) or 0.2% v/v poly(ethylene glycol) 1000 (for N170M), 0.3 M KCl, and 0.1 M $NaHCO_3$ buffered at pH 8. The hanging drops contained equal volumes of enzyme solutions (10−13 mg/mL) and reservoir solutions. The crystals belong to space group *I*222 (Table 2) and are isomorphous with the crystals of the native enzyme (Herzberg & Moult, 1987).

X-ray intensity data were collected at room temperature on a Siemens area detector mounted on a Siemens 3-axis goniostat. Focusing mirror-monochromated Cu Kα X-rays were generated by a Siemens rotating anode. The data were processed with the XENGEN package (Howard et al., 1987). The statistics of data processing are shown in Table 2.

Structure Determination and Refinement. The crystals of both mutant enzymes were isomorphous with the native crystals. Hence, the starting model for refinement was that of the native *S. aureus* PC1 β-lactamase (Protein Data Bank entry code 3BLM), except that the amino acid residue at position 170 was truncated to an alanine. The structure factors were scaled to absolute values with the computer program ORESTES written by W. E. Thiessen and H. A. Levy. The structures were refined with the computer program package X-PLOR (Brünger et al., 1987), following the positional refinement and temperature factor refinement protocols. Map inspection and manual adjustments were made using the interactive graphics program TURBO-FRODO (Roussel & Cambillau, 1989). Two types of electron density maps with the coefficients $2|F_o| - |F_c|$ and $|F_o| - |F_c|$ and with calculated phases were inspected simultaneously. The electron density maps after the initial positional refinement revealed that the expected larger side chains of the mutated amino acid were present. These were incorporated into the models, and refinement was resumed with the complete protein model. Solvent molecules were added to the models once the *R*-value reached 0.241 for the N170Q enzyme and 0.205 for the N170M enzyme ($R = \sum_h ||F_o| - |F_c|| / \sum_h |F_o|$, where $|F_o|$ and $|F_c|$ are the observed and calculated structure factor amplitudes, respectively). These were assigned using the $|F_o| - |F_c|$ difference Fourier maps with 3σ level cutoff criteria.

Table 3: Refinement Statistics

	N170Q	N170M
resolution range (Å)	8.0−2.2	8.0−2.0
no. of unique reflections, $F \geq 2\sigma(F)$	15046	16582
R[a]	0.179	0.156
no. of amino acid residues	257	257
no. of water molecules	219	162
rmsd from ideal geometry		
bond length (Å)	0.021	0.019
bond angles (deg)	2.0	1.9

[a] $R = \sum_h ||F_o| - |F_c|| / \sum_h |F_o|$, where $|F_o|$ and $|F_c|$ are the observed and calculated structure factor amplitudes, respectively.

RESULTS AND DISCUSSION

Refinement Results. The refinement statistics of the two mutant enzymes are summarized in Table 3. The electron density maps associated with the sites of the mutations are shown in Figure 1. The electron density at the region of the N-terminal methionine, inserted for expression purposes, is not sufficiently clear for tracing. Within the experimental error, the overall structures are identical to that of the native enzyme. When the models of each of the mutant enzymes are superimposed on that of the native enzyme, the root-mean-square (rms) deviations are 0.1 and 0.2 Å for the α-carbon atoms of the N170M and N170Q enzymes, respectively. For all atoms, the corresponding values are 0.4 and 0.6 Å, with the largest coordinate differences corresponding to a few side chains of surface lysine residues.

The most significant structural difference is associated with the additional volume of the mutated side chain at position 170, and the two mutant enzymes differ from each other (Figure 2). The side chain of Gln170 extends toward the site of the proposed hydrolytic water molecule (Wat2), and there is no electron density in the niche consistent with the presence of such a water molecule. It should be noted though that, because of the limited accuracy of the structure determination, partial occupancy of the site of the order of 10−20% would not be detectable in the electron density map. The side chain of Met170 protrudes into the active site depression, occupying space that in the native structure is available for the substrate. Electron density consistent with the presence of a water molecule is apparent in the niche flanked by Glu166, Ser70, and Met170 (Figure 1). Except for the mutation site, the conformations of all the key catalytic residues and the position of the water molecule that occupies the oxyanion hole (Wat1) are essentially the same in both mutant molecules as in the native structure.

Kinetic Characterization. Mechanistic studies have established the simplest reaction scheme for the serine β-lactamases as shown in Scheme 1 (Knott-Hunziker et al., 1979; Cartwright & Coulson, 1980; Cohen & Pratt, 1980; Fisher et al., 1980). In this scheme the enzyme, substrate, and product are depicted by E, S, and P, respectively, ES corresponds to the Michaelis complex, and EC corresponds to the acyl enzyme complex. The acylation step is considered irreversible, a reasonable approximation if the deacy-

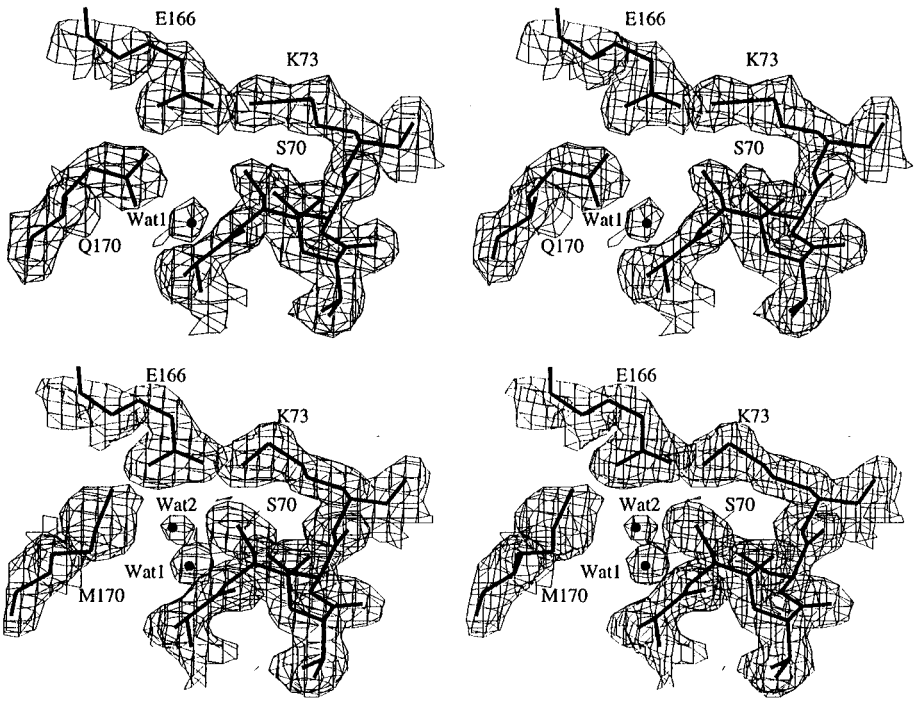

FIGURE 1: Stereoscopic representation of the electron density maps in the regions of the mutations, displayed together with the protein model. The maps are calculated with the coefficients $2F_o - F_c$ and contoured at the 1σ level. (a, top) N170Q β-lactamase. (b, bottom) N170M β-lactamase.

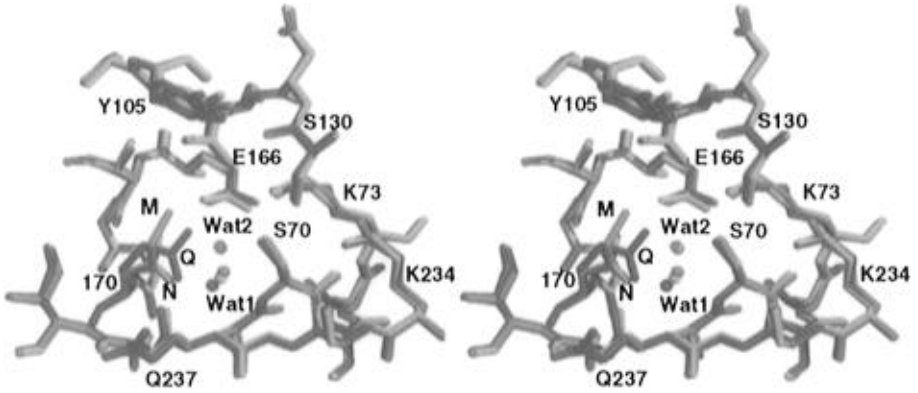

FIGURE 2: Stereoscopic view of the superposition of the active sites of the native (gold), N170Q (red), and N170M (blue) β-lactamases. The water molecule that occupies the oxyanion hole is labeled Wat1 and is present in all three structures. The proposed hydrolytic water molecule is labeled Wat2 and is missing in the structure of the N170Q mutant enzyme.

Scheme 1

$$E + S \overset{K_s}{\Longleftrightarrow} ES \overset{k_2}{\longrightarrow} EC \overset{k_3}{\longrightarrow} E + P$$

lation step is fast. Kinetics studies of β-lactamase have also revealed a more complex reaction termed substrate-induced inactivation or branched pathway. This usually occurs when the enzyme interacts with the so-called A-type substrates (Citri et al., 1976; Pain & Virden, 1979; Waley, 1991). Several schemes have been described for the branched pathway (Waley, 1991), but the most commonly discussed is shown in Scheme 2. Here, the initial acyl enzyme, EC,

Scheme 2

$$E + S \overset{K_s}{\Longleftrightarrow} ES \overset{k_2}{\longrightarrow} EC \overset{k_3}{\longrightarrow} E + P$$
$$\underset{k_{-4}}{\overset{k_4}{\Updownarrow}}$$
$$EC^*$$

is converted to a second form of an acyl enzyme, EC*, which does not turn over (or turns over more slowly). The progress curve exhibits an initial exponential phase followed by a slower steady-state linear phase. Usually, the initial burst of product is much greater than the concentration of the enzyme. The product formation can be described by the equation:

$$P = v_s t - (v_s - v_i)(1 - e^{-kt})/k \qquad (1)$$

where P is the concentration of the product at time t, v_i is the initial velocity, v_s is the steady-state velocity, and k is the rate constant characterizing the change. The branched pathway may be contrasted with a progress curve that follows Scheme 1, in the case where $k_2 \gg k_3$. A fast burst with the amplitude that equals 1 mol of product/mol of enzyme is characteristic of this mechanism, if the acyl enzyme and the product absorb light similarly. The apparent steady-state rate, k_{cat}, is then equivalent to k_3, the rate of deacylation. In addition, Fink et al. (1994) discussed the case in which $k_3 < k_4$ in a branched pathway, a condition that may also lead to a burst with amplitude of 1.

Table 4: Hydrolysis Parameters for N170Q and N170M β-Lactamases

substrate	parameter	N170Q	N170M	wild-type
benzylpenicillin	k_{cat} (s^{-1})	0.0094 ± 0.0005	0.0118 ± 0.0006	120 ± 2
FAP	k_{cat} (s^{-1})	0.027 ± 0.002	0.22 ± 0.01	184 ± 3
	burst stoichiometry	2.5	8	
nitrocefin	v_s[a] or k_{cat} (s^{-1})	0.0144 ± 0.0002	0.22 ± 0.01	11.4[b]
	v_i[a] (s^{-1})		2.31 ± 0.12	
	k[a] (s^{-1})		0.0166 ± 0.0001	
	burst stoichiometry	1.2	70	
	K_m (μM)	<1	55.2 ± 8.1	6.9[b]

[a] Rates from fitting to the burst equation: $P = v_s t - (v_s - v_i)(1 - e^{-kt})/k$ (Waley, 1991). [b] Previously reported (Herzberg et al., 1991).

Native *S. aureus* PC1 β-lactamase undergoes simple acylation/deacylation reactions with the S-type substrates benzylpenicillin, the chromogenic penicillin, 6-β-[(furylacryloyl)amido]penicillanic acid (FAP), and the chromogenic cephalosporin, nitrocefin. The use of the latter two substrates is advantageous because of their absorption in wavelength regions where there is little absorption by the protein. Nitrocefin is particularly attractive because of the large absorption change that accompanies the opening of the β-lactam ring. These substrates were used in this study, in addition to the traditional substrate benzylpenicillin. The absorption of the acyl enzyme is usually assumed to be similar to that of the hydrolyzed substrate, an assumption that may not be entirely correct.

The catalytic rates of benzylpenicillin hydrolysis with both mutant enzymes are about 10^4 lower compared with the rate of the native enzyme (Table 4). Pre-steady-state burst cannot be reliably identified because the extinction coefficient of benzylpenicillin is rather low and is monitored at 232 nm, a wavelength where the protein absorption is appreciable. It was impossible to determine whether the N170Q mutant enzyme exhibits burst kinetics, although there was an indication of a progress curve that follows a branched pathway with the N170M mutant enzyme.

Unequivocal results were obtained by monitoring nitrocefin hydrolysis. The N170Q β-lactamase exhibits a fast burst with stoichiometry of 1 mol of product/mol of enzyme, assuming the same extinction coefficient for the acyl enzyme as for the hydrolyzed nitrocefin. This is followed by a steady-state hydrolysis rate which is 800-fold slower than the rate of the native enzyme (Figure 3a, Table 4). The K_m value is lower than 1 μM and could not be accurately determined because of the high enzyme concentrations required to follow the reaction.

To attempt to distinguish between a simple linear mechanism (Scheme 1) and the branched pathway (Scheme 2), the reaction was monitored in the presence of 0.5 M ammonium sulfate. Mitchinson and Pain (1985) have shown that sulfate stabilizes the native form of β-lactamase from *S. aureus*; hence it was expected that for a branched pathway the burst stoichiometry would increase. A similar experiment has been done with the E166C β-lactamase from *B. licheniformis*, for which a doubling of the burst stoichiometry was observed in the presence of 0.5 M ammonium sulfate (Escobar et al., 1994). This was interpreted as indicative of a branched pathway. For the N170Q β-lactamase in the current study, the burst amplitude was identical to that observed in sulfate-free solutions. Hence, there is no evidence to support branched pathway kinetics in this case. Interestingly, $k_{cat} = 0.035$ s^{-1}, a 2.5-fold increase compared with the rate in a sulfate-free solution.

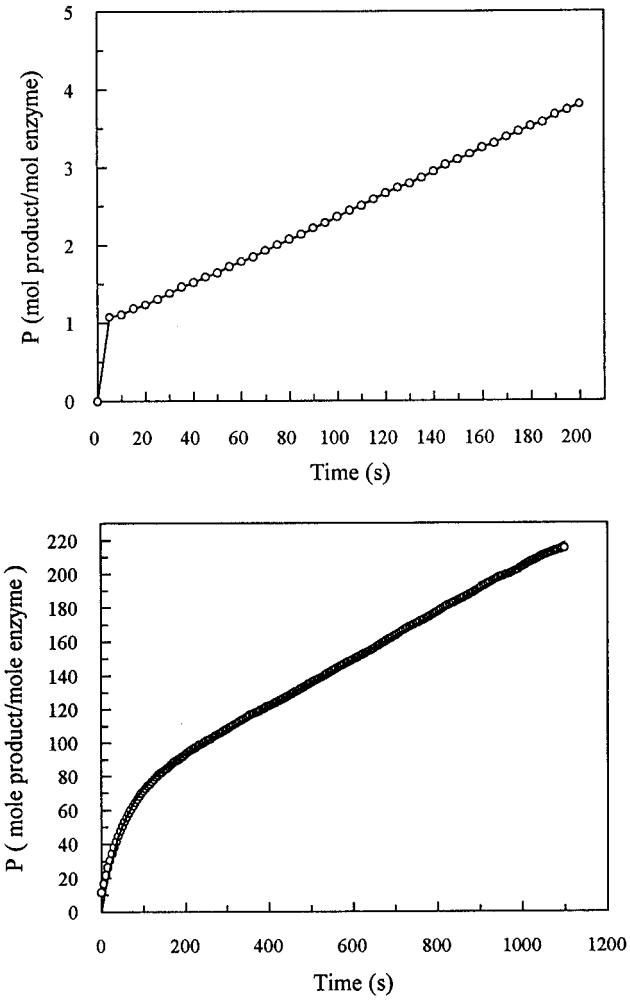

FIGURE 3: Progress curves of nitrocefin hydrolysis. (a, top) N170Q β-lactamase exhibits a burst with a stoichiometry of approximately 1 mol of product/mol of enzyme followed by a linear phase. The concentration of enzyme and the initial concentration of nitrocefin were 0.9 and 63 μM, respectively. (b, bottom) N170M β-lactamase exhibits a slow progressive inactivation followed by a linear phase, indicative of a branched pathway mechanism. The stoichiometry of the burst is approximately 70 mol of product/mol of enzyme. The circles correspond to the measured data, and the line is that resulting from fitting to the equation $P = v_s t - (v_s - v_i)(1 - e^{-kt})/k$ (Waley, 1991). The assay was performed with 0.12 μM enzyme and 94 μM nitrocefin.

For the N170M mutant enzyme, a slow pre-steady-state burst is observed with a stoichiometry of 70:1 between the product and the enzyme (Figure 3b). This is followed by an apparent steady-state phase. Accordingly, the progress curves were fitted with the burst equation (Waley, 1991). The steady-state hydrolysis rate is 52-fold lower and the K_m value is 10-fold higher compared with the values for the native enzyme (Table 4).

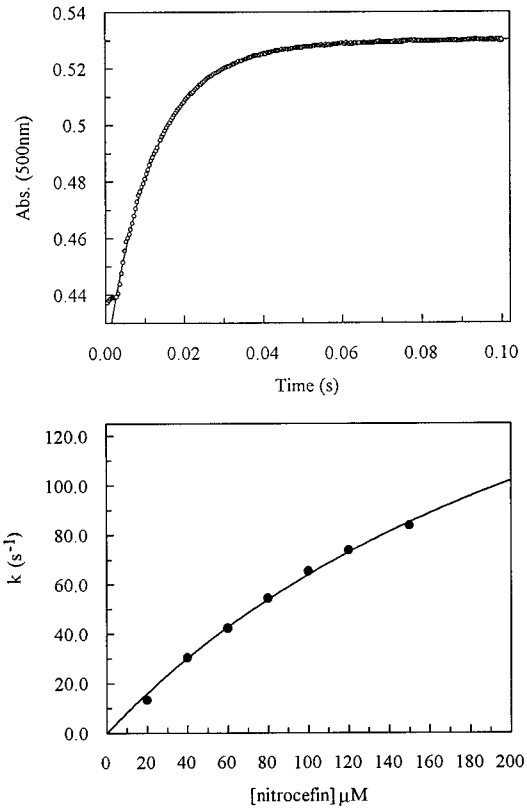

FIGURE 4: Stopped-flow kinetics of the hydrolysis of nitrocefin by N170Q β-lactamase. (a, top) A curve representing the average of four progress curves at the maximum nitrocefin concentration used, 150 μM. The enzyme concentration was 2.95 μM throughout. The circles represent the measured data, and the overlaid line corresponds to the fit to the exponential equation (eq 2). The first data points were excluded from the analysis because of mixing artifacts. Only 0.1 s of the total of 1 s that was monitored is shown in order to highlight the exponential part of the curve. The amplitude of the exponential component equals 0.111 and corresponds to 1 mol of degraded nitrocefin/mol of enzyme. (b, bottom) The rate constant k as a function of nitrocefin concentration. The substrate concentrations ranged between 20 and 150 μM. Each concentration point was derived by averaging four to ten experiments. The curve corresponds to the fit to a hyperbolic equation: $k = k_2[S]/(K_s + [S])$.

To determine the rate of acylation for the N170Q β-lactamase, pre-steady-state kinetic experiments have been performed in the stopped-flow apparatus, under excess nitrocefin concentrations. The enzyme concentration was 3 μM enzyme and the nitrocefin concentration ranged from 20 to 150 μM. Seven substrate concentrations were used, and, for each, four to ten measurements were made and averaged. The reactions were monitored for 1 s. The data were fitted to the equation:

$$[P]_{obs} = [EC] + [P] = A(1 - e^{-kt}) + k_{cat}t \qquad (2)$$

where EC is the acyl enzyme and P is the hydrolyzed nitrocefin, A represents the exponential phase amplitude, k is the burst rate constant, k_{cat} is the steady-state rate, and t is time. An example of a progress curve is shown in Figure 4a. Consistent with the steady-state result, the stoichiometry of enzyme and the degraded nitrocefin during the burst is 1:1.

Over the concentration range of nitrocefin, the value of k increased in a hyperbolic fashion without reaching its maximum. The data were fitted to the equation:

$$k = k_2[S]/(K_s + [S]) \qquad (3)$$

where [S] is the nitrocefin concentration, k_2 is the apparent acylation rate, and K_s is the apparent substrate dissociation constant (Figure 4b). The resulting apparent rate constants were

$$k_2 = 252 \pm 29\ s^{-1} \quad \text{and} \quad K_s = 300 \pm 20\ \mu M$$

The stopped-flow kinetics also confirm that for the N170Q β-lactamase $k_{cat} \ll k_2$. Previous work has shown the rate of acylation of nitrocefin, k_2, for the native β-lactamase to be approximately 200 s^{-1} (Herzberg et al., 1991). Clearly, the N170Q β-lactamase exhibits a rate of acylation comparable to that of the native enzyme.

The chromogenic penicillin, FAP, has a distinctive chromophore in the 320−350 nm wavelength range. The loss of FAP absorption at 344 nm was monitored, where absorption by the enzyme is very low. The k_{cat} value of native β-lactamase with FAP is quite comparable to that with benzylpenicillin (Table 4), and the k_{cat} values for the N170Q and N170M β-lactamases are reduced by approximately 4 and 3 orders of magnitude, respectively. In addition, a fast burst is visible with both mutant enzymes. Assuming similar extinction coefficients for the acyl enzyme and the product, the stoichiometry of the burst was approximately 2.5 mol of product/mol of enzyme for the N170Q mutant enzyme and 8 for the N170M mutant enzyme. Unlike the nitrocefin result, the 1:2.5 stoichiometry of the N170Q mutant enzyme with FAP appears inconsistent with simple slowing of deacylation. There may be two explanations for this. Either there is involvement of a branched pathway mechanism or the extinction coefficient of the acyl enzyme for this substrate differs from that of the product. Modeling shows that, in contrast to the chromogenic group of nitrocefin that is likely to be fully solvated when bound to the enzyme, the chromogenic side chain of FAP appears to interact with the active site gully in a manner similar to that observed in the crystal structure of a phosphonate/enzyme complex (Chen et al., 1993). In that complex, there are extensive contacts with several hydrophobic residues and with a tyrosine side chain. Such a partially desolvated environment would be expected to affect the spectrum of the furylacryloyl moiety.

Mechanistic Implications. The kinetic data for the N170Q β-lactamase indicate that its deacylation machinery is severely impaired. The kinetics should be considered in the context of the crystal structure that reveals that Glu166 is present in the same conformation as in the native structure but the water molecule adjacent to it is missing. The site of the water molecule is partially occupied by the side chain of the engineered Gln170. No other changes are observed in the active site; hence the reduction in the hydrolysis rate is attributed to the elimination of the water molecule. Two structurally based mechanisms are envisaged as possibly giving rise to the kinetic characteristics. In the first, an infrequent conformational adjustment of the side chain of Gln170, with the amido group shifted away from the water molecule site, may occur but would not be detectable in the electron density map. For these molecules, the water molecule would occupy the site that enables deacylation. The rate constants may or may not be similar to those of the wild-type enzyme. The kinetic scheme that describes this catalytic process is shown in Scheme 3. Here E′ is the

Scheme 3

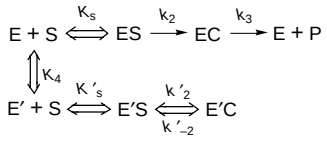

enzyme conformation lacking the proposed hydrolytic water molecule, and E is the enzyme conformation with the water molecule bound as in the native structure. Accordingly, E′C corresponds to an acyl enzyme intermediate that is deacylation defective and EC to the infrequently sampled acyl enzyme capable of deacylation. EC and E′C are spectroscopically indistinguishable. The 1:1 burst stoichiometry represents both forms, and the measured acylation rate and the dissociation constant are composite rates of both reactions. In addition, because E′C does not undergo deacylation, the reversibility of its acylation step cannot be ignored. If acylation and deacylation of EC are comparable with those of the wild-type enzyme, the overall catalytic rate is determined by the partition between the two forms of the enzyme (K_4) and by the rate of the reverse acylation reaction (k'_{-2}).

On the other hand, if one assumes that the niche for the proposed hydrolytic water molecule is always blocked by Gln170, an alternative mechanism must be invoked. In that case, the hydrolytic water molecule is provided by the bulk solvent, following the formation of the acyl enzyme. The substrate moiety acquires additional flexibility because of the opening of the β-lactam ring and can reorient to relieve the crowding at the site where originally the β-lactam nitrogen atom was placed (close to Ser130). This implies a nucleophilic attack that occurs from the opposite direction compared with that envisaged for Wat2 in the native structure. The direction of attack is analogous to that proposed in the mechanism of the serine proteases and also that implied by the proposed mechanism of the class C β-lactamases (Oefner et al., 1990; Lobkovsky et al., 1994). The caveat is that a serine residue is less likely to activate a water molecule for a nucleophilic attack compared with the hydroxyl group of a tyrosine of the class C enzymes, hence the slow deacylation. The kinetic scheme that describes this process is shown in Scheme 4. Here EC′ is the acyl enzyme

Scheme 4

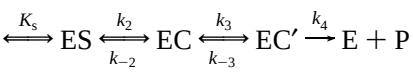

in which the substrate has undergone an orientational adjustment, enabling a bulk water molecule to attack the carbonyl carbon of the ester linkage. For this mechanism k_4 is the rate-limiting step and $k_{cat} = k_4$. As deacylation is slow, the reversibility of the acylation step cannot be ignored. By contrast with the simple linear Scheme 1, for which $k_{cat}/K_m = k_2/K_s$, k_{cat}/K_m according to Scheme 4 is a function of all the rate constants including k_4, and k_2 may still be as fast as with the wild-type enzyme.

Both of the above proposed mechanisms imply that the N170Q β-lactamase is deacylation-impaired because of the missing hydrolytic water molecule and that, in the wild-type enzyme, nucleophilicity is enhanced by Glu166. In contrast, the crystal structure of the N170M mutant enzyme reveals that the proposed hydrolytic water is present and the side chain of Met170 occupies part of the space required for substrate binding. While the machinery for hydrolysis is intact, substrate affinity is expected to be reduced because of the interference of the methionine side chain. This is seen by the increased K_m value compared with that of the wild-type enzyme. Modeling shows that short contacts would occur between Met170 and the side chain substituent of the β-lactam. As Met170 resides on the Ω-loop, a potentially flexible polypeptide segment (Herzberg & Moult, 1987; Herzberg, 1991), conformational changes may be expected. These would be accompanied by branched pathway kinetics because Glu166, also located on the Ω-loop, would be displaced. This rationale pertains also to cases in which access to the active site depression is restricted for β-lactams with bulky side chain substituents (i.e., A-type substrates). Such substrates exhibit kinetics that are consistent with a branched pathway (Citri et al., 1976; Pain & Virden, 1979).

Implications to the Role of Glu166 and Lys73 in Catalysis. The fast acylation rate of N170Q β-lactamase, comparable with that of the native enzyme, together with the slow catalytic rate discredits the proposal that during acylation Glu166 accepts the proton from Ser70′s hydroxyl group via the water molecule (Damblon et al., 1996). Could Glu166 have another role in acylation? It has been proposed that Lys73 is deprotonated and accepts the proton from Ser70 during the acylation step (Strynadka et al., 1992). On the other hand, NMR data for the related β-lactamase from *E. coli* show that Lys73 is positively charged in the free enzyme (Damblon et al., 1996). A possible role for Glu166 would therefore be to assist in deprotonation of Lys73 upon desolvation of the active site by the substrate. The neutral lysine could then accept a proton from Ser70 and subsequently transfer it to the β-lactam nitrogen atom. However, this does not seem to be an essential role for Glu166 as the mutant enzymes with uncharged residues at position 166 are still capable of acylation (Adachi et al., 1991; Escobar et al., 1991). Either the pK_a of Lys73 is dramatically reduced upon substrate binding without assistance from Glu166 or Lys73 cannot provide a proton park in the classical manner of a general base. Perhaps these two alternatives could be resolved by determining the pK_a of Lys73 in the presence of substrate.

ACKNOWLEDGMENT

We thank Philip Bryan for help and advice with the stopped-flow kinetic experiments and Edward Eisenstein and Rex Pratt for helpful discussions.

REFERENCES

Adachi, H., Ohta, T., & Matsuzawa, H. (1991) *J. Biol. Chem. 266*, 3186−3191.

Ambler, R. P. (1980) *Philos. Trans. R. Soc. London B289*, 321−331.

Ambler, R. P., Coulson, A. F. W, Frère, J.-M., Ghuysen, J.-M., Joris, B., Forsman, M., Levesque, R. C., Tiraby, G., & Waley, S. G. (1991) *Biochem. J. 276*, 269−270.

Brünger, A. T., Kuriyan, J., & Karplus, M. (1987) *Science 235*, 458−460.

Carrey, E. A., & Pain, R. H. (1978) *Biochim. Biophys. Acta 533*, 12−22.

Cartwright, S. J., & Coulson, A. F. W. (1980) *Philos. Trans. R. Soc. London B289*, 370−372.

Chen, C. C. H., & Herzberg, O. (1992) *J. Mol. Biol. 224*, 1103−1113.

Chen, C. C. H., Rahil, J., Pratt, R. F., & Herzberg, O. (1993) *J. Mol. Biol. 234*, 165−178.
Chen, C. C. H., Smith, T. J., Kapadia, G., Wäsch, S., Zawadzke, L. E., Coulson, A., & Herzberg, O. (1996) *Biochemistry 35*, 12251−12258.
Citri, N., Samuni, A., & Zyk, N. (1976) *Proc. Natl. Acad. Sci. U.S.A. 73*, 1048−1052.
Cohen, S. A., & Pratt, R. F. (1980) *Biochemistry 19*, 3996−4003.
Damblon, C., Raquet, X., Lian, L.-Y., Lamotte-Brasseur, J., Fonze, E., Charlier, P., Roberts, G. C. K., & Frère, J.-M. (1996) *Proc. Natl. Acad. Sci. U.S.A. 93*, 1747−1752.
Escobar, W. A., Tan, A. K., & Fink, A. L. (1991) *Biochemistry 30*, 10783−10787.
Escobar, W. A., Tan, A. K., Lewis, E. R., & Fink, A. L. (1994) *Biochemistry 33*, 7619−7626.
Fisher, J., Belasco, J. G., Kohsla, S., & Knowles, J. R. (1980) *Biochemistry 19*, 2895−2901.
Gibson, R. M., Christensen, H., & Waley, S. G. (1990) *Biochem. J. 272*, 613−619.
Herzberg, O. (1991) *J. Mol. Biol. 217*, 701−719.
Herzberg, O., & Moult, J. (1987) *Science 236*, 694−701.
Herzberg, O., & Moult, J. (1991) *Curr. Opin. Struct. Biol. 1*, 946−953.
Herzberg, O., Kapadia, G., Blanco, B., Smith, T., & Coulson, A. F. W. (1991) *Biochemistry 30*, 9503−9509.
Ho, S. N., Hunt, H. D., Horton, R. M., Pullen, J. K., & Pease, L. R. (1989) *Gene 77*, 51−59.
Howard, A. J., Gilliland, G. L., Finzel, B. C., Poulos, T., Ohlendorf, D. O., & Salemme, F. R. (1987) *J. Appl. Crystallogr. 20*, 383−387.
Jelsch, C., Lenfant, F., Masson, J. M., & Samama, J. P. (1992) *FEBS Lett. 299*, 135−142.
Jelsch, C., Mourey, L. F., Masson, J. M., & Samama, J. P. (1993) *Proteins 16*, 364−383.
Knott-Hunziker, V., Waley, S. G., Orlek, B. S., & Sammes, P. G. (1979) *FEBS Lett. 99*, 59−61.
Knox, J. R., & Moews, P. C. (1991) *J. Mol. Biol. 220*, 435−455.
Lamotte-Brasseur, J., Dive, G., Dideberg, O., Charlier, P., Frère, J.-M., & Ghuysen, J.-M. (1991) *Biochem. J. 279*, 213−221.
Lobkovsky, E., Moews, P. C., Liu, H., Zhao, H., Frère, J.-M., & Knox, J. R. (1993) *Proc. Natl. Acad. Sci. U.S.A. 90*, 11257−11261.
Lobkovsky, E., Billing, E. M., Moews, P. C., Rahil, J., Pratt, R. F., & Knox, J. R. (1994) *Biochemistry 33*, 6762−6772.
Mitchinson, C., & Pain, R. H. (1985) *J. Mol. Biol. 184*, 331−342.
Moews, P. C., Knox, J. R., Dideberg, O., Charlier, P., & Frère, J.-M. (1990) *Proteins 7*, 156−171.
Monnaie, D., Dubus, A., & Frère, J. M. (1994) *Biochem. J. 302*, 1−4.
Oefner, C., D'Arcy, A., Daly, J. J., Gubernato, K., Charnas, R. L., Heinze, I., Hubschwerlen, C., & Winkler, F. K. (1990) *Nature 343*, 284−288.
Pain, R. H., & Virden, R. (1979) in *Beta-Lactamases* (Hamilton-Miller, J. M. T., & Smith, J. T., Eds.) pp 141−180, Academic Press, London.
Roussel, A., & Cambillau, C. (1989) *Silicon Graphics Geometry Partners Directory*, pp 77−78, Silicon Graphics, Mountain View, CA.
Strynadka, N. C. J., Adachi, H., Jensen, S. E., Johns, K., Sielecki, A., Betzel, C., Sutoh, K., & James, M. N. G. (1992) *Nature 359*, 700−705.
Tsukamoto, K., Tachibana, K., Yamazaki, N., Ishii, Y., Ujiie, K., Nishida, N., & Sawai, T. (1990) *Eur. J. Biochem. 188*, 15−22.
Waley, S. G. (1991) *Biochem. J.* 279, 87−94.
Zawadzke, L. E., Smith, T., & Herzberg, O. (1995) *Protein Eng. 8*, 1275−1285.

BI962242A